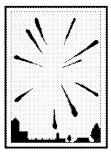

*Meteoritics & Planetary Science* 38, Nr 6, 887–893 (2003)
Abstract available online at http://meteoritics.org

# $^{40}Ar/^{39}Ar$ laser probe dating of the Central European tektite-producing impact event

Marinella A. LAURENZI,[1*] Giulio BIGAZZI,[1] Maria Laura BALESTRIERI,[1] and Vladimìr BOUŠKA[2]

[1]Istituto di Geoscienze e Georisorse, Area della Ricerca CNR, Via G. Moruzzi, 1, 56124 Pisa, Italy
[2]Institute of Rock Structure and Mechanics, Academy of Sciences, Prague, Czech Republic
[*]Corresponding author. E-mail: m.laurenzi@igg.cnr.it

*(Received 20 November 2002; revision accepted 7 March 2003)*

**Abstract**–A new $^{40}Ar/^{39}Ar$ data set is presented for tektites from the Central European strewn field (moldavites). This is the only strewn field that is entirely situated in a continental environment and still characterized by scattered ages (14–15.3 Myr). The main objectives of the study were to define more precisely the moldavite formation age and provide a good calibration for a glass standard proposed for fission-track dating.

The laser total fusion ages obtained on chips from 7 individual specimens from the Southern Bohemian and Moravian subfields are restricted to a narrow interval of time, with an average of 14.34 ± 0.08 Myr relative to the 27.95 ± 0.09 Myr of the Fish Canyon Tuff biotite. This result gives a more precise age not only for the tektite field but also for its producing impact. If the genetic link between the moldavites and the Nördlinger Ries impact crater is maintained, then this new age has to be considered a reliable estimate for the Ries crater also.

This new value places the formation of Central European tektites within the Lower Serravallian period in the latest geologic timescales. Evidence of their impact products, such as glass spherules or shocked minerals, can, therefore, be sought in sedimentary marine formations in a more precisely defined age interval.

## INTRODUCTION

Tektites are natural silicate glasses that can be found in only 4 "classic" strewn fields in North America, Central Europe, the Ivory Coast, and Australasia. Other impact-related glasses are often referred to as tektites, but so far, only the historical tektites are considered as such (see Dressler and Reimold [2001] for a thorough review on impact glasses). Tektites are characterized by very low water and volatile contents, and overall chemical data indicate that they were probably formed by hypervelocity impact melting of terrestrial sediments (Koeberl 1994). Tektite formation requires very strict boundary conditions that are still largely unknown because strewn fields are far less numerous than known impact craters (Grieve 1997). The K/Ar (and its variant $^{40}Ar/^{39}Ar$) and fission-track (FT) methods are used widely for dating tektites, and, indeed, the latter were among the first products to be dated with the K/Ar method (Suess et al. 1951).

Moldavites are the tektites found in sedimentary deposits of various ages in Central Europe: the majority of moldavite finds come from Southern Bohemia (80.4%) and Moravia (19.5%), with only a few specimens from Lusatia (Germany) and north-eastern Austria (Bouška 1998). They form the only strewn field that is entirely confined to a continental environment. Moldavites were never found in situ but only as transported or even reworked materials embedded in sediments spanning about 12 Myr, from the Middle Miocene to the Holocene; hence, they lack the strict chronostratigraphic control that is often observed on microtektites found in situ in marine deposits. The ages reported in the literature for this strewn field are spread over a wide interval of time (14–15.3 Myr) (Storzer et al. 1995), and the majority were obtained with the K/Ar and fission-track methods in the 1960s (Gentner et al. 1963; Zähringer 1963; Gentner et al. 1967; McDougall and Lovering 1969). The few published $^{40}Ar/^{39}Ar$ plateau ages differ slightly (15.21 ± 0.15 Myr [Staudacher et al. 1982] and 14.4 ± 0.25 Myr [Lange et al. (1995), recalculated to 14.52 ± 0.40 Myr (2σ) due to a revision of monitor age in Schwarz and Lippolt (2002)]) or are affected by an error of about 2 Myr (Mader et al. 2001). In a recent paper, Schwarz and Lippolt (2002) report a younger mean $^{40}Ar/^{39}Ar$ plateau age on moldavites from the Bohemian and Lusatian strewn field: 14.50 ± 0.42 Myr and 14.38 ± 0.24

Myr, respectively, with errors at the 2σ level. The interval of variation of these ages is too large considering the state of the art of modern geochronology and when compared with data on other strewn fields.

The Subcommission on Geochronology of the International Union of Geological Sciences (IUGS) included moldavites in its list of potential age standards for FT dating (Hurford 1990). Moldavites are considered to be a peculiar glass that is generally unaffected by track annealing, which is very common in volcanic glasses and results in lower ages. A better definition of moldavite age is a necessary prerequisite for its use as a reference glass.

## ANALYTICAL DATA

### Samples

The $^{40}Ar/^{39}Ar$ study was made on 7 samples collected by one of the authors (V. Bouška), with different stratigraphic ages and FT behaviors (Table 1). Two ferrous moldavites from the Jankov deposit and one each from the Vrábče, Chlum nad Malší, and Třebanice deposits represent the Southern Bohemia strewn subfield. The Radomilice sample is representative of a small subfield of the Southern Bohemia strewn subfield, while the reworked Slavice moldavite is from the Moravian subfield. Jankov is the deposit with the oldest stratigraphic age (Lower Sarmatian, about 12 Myr) and contains the moldavite with the lowest amount of fission-track annealing (Bouška et al. 2000). Chlum nad Malší and Třebanice are from Pliocenic deposits, Vrábče is from a Middle Miocenic deposit, and Radomilice is from a Plio-Pleistocenic deposit. They all show the same amount of track annealing in FT dating, but Chlum nad Malší and Radomilice are rounded moldavites, which is indicative of a longer pre-deposition geologic history (Bouška et al. 2000). The Slavice moldavite is from a Miocene deposit, reworked in the Plio-Pleistocene. It yielded a very low apparent FT age and showed a bimodal spontaneous track-size distribution, indicating a complex thermal history (Balestrieri et al. 1998).

### $^{40}Ar/^{39}Ar$ Dating

$^{40}Ar/^{39}Ar$ analyses were performed on a single moldavite specimen that had previously undergone FT dating (Bigazzi and De Michele 1996; Balestrieri et al. 1997; Balestrieri et al. 1998; Bouška et al. 2000); the original weight of the samples is reported in Table 1. Pieces of green moldavites were lightly crushed in an agate mill, and small chips with no visible bubbles or surface alteration were selected under a microscope for analysis. The samples were wrapped in Al foil to form disks, piled up inside a quartz tube (9 mm in diameter), and irradiated for 10 (PAV-49) and 8 hours (PAV-51) in the thimble of the 250 kW TRIGA reactor at Pavia University. Vertical neutron flux variations were monitored with Fish Canyon Tuff biotite split 3 (FCTb) (1 standard for every 3 samples: equivalent to 1 standard every ~5 mm) with an assigned age of 27.95 Myr ± 0.09 Myr (1σ) (Baksi et al. 1996). No data are available on ~1 mg sizes of FCT biotite, which means its homogeneity is unknown on a very small scale. A check was done by analyzing double splits of about 1.5 mg for each monitor, step-heated by means of a defocused laser beam. The integrated $^{40}Ar_{rad}/^{39}Ar_K$ ratios obtained from summing all the steps were equal within analytical error (on average 0.3% at the 2σ level) for the 2 splits.

Individual chips of different sizes were loaded into 2.5 mm diameter holes drilled into a copper sample holder and were melted using a focused continuous wave Nd-YAG infrared laser (~40 W maximum power). The evolved gas was cleaned by 2 AP-10 SAES getters held at ~280° and ~400°C and analyzed with a MAP215–50® mass spectrometer using a secondary electron multiplier as the collector. Step-heating experiments were performed on some samples using a defocused (i.e., broadened) laser beam, but melting the samples at this setting was impossible. After a few steps with a limited release of K-derived $^{39}Ar$, the grains started to lose their shape and amalgamated into one sphere that started to contract slowly as the laser power increased; a focused laser beam was, however, needed to melt the sample and release most of the gas. This behavior was independent of the grain

Table 1. Stratigraphic and isotopic age data of analyzed samples.[a]

| Sample | Stratigraphic age | Avg. ± std. dev. (Myr) | Wa ±1σ (Myr) | MSWD | Is. age ±1σ (Myr) | MSWD | Tot. age ±1σ (Myr) | SH total age ±1σ (Myr) |
|---|---|---|---|---|---|---|---|---|
| Jankov #1 (5.608 g) | MM | 14.27 ± 0.08 | 14.24 ± 0.07 | 2.68 | 14.22 ± 0.08 | 2.8 | 14.26 ± 0.07 | 14.28 ± 0.07 |
| Jankov #2 (12.69 g) | MM | 14.31 ± 0.07 | 14.31 ± 0.07 | 15.07 | 14.64 ± 0.11 | 2.8 | 14.32 ± 0.07 | 14.33 ± 0.07 |
| Slavice (11.376 g) | MM | 14.29 ± 0.07 | 14.28 ± 0.07 | 3.47 | 14.27 ± 0.07 | 3.3 | 14.30 ± 0.07 | 14.29 ± 0.07 |
| Chlum (6.338 g) | P | 14.32 ± 0.05 | 14.30 ± 0.08 | 2.52 | 14.13 ± 0.14 | 0.4 | 14.30 ± 0.07 | 14.36 ± 0.07 |
| Třebanice (4.399 g) | P | 14.42 ± 0.05 | 14.43 ± 0.07 | 3.16 | 14.27 ± 0.10 | 0.8 | 14.43 ± 0.07 | |
| Radomilice (3.174 g) | PP | 14.40 ± 0.11 | 14.43 ± 0.08 | 8.45 | 14.40 ± 0.08 | 5.6 | 14.40 ± 0.07 | |
| Vrábče (1.812 g) | MM | 14.38 ± 0.06 | 14.38 ± 0.07 | 3.87 | 14.36 ± 0.07 | 3.8 | 14.38 ± 0.07 | |
| Average ± std. dev. | | 14.34 ± 0.06 | 14.34 ± 0.08 | | | | 14.34 ± 0.06 | |

[a]Each sample name is followed by the weight of the original specimen in grams. Abbreviations in column headings are: Avg. ± std. dev. = average ± standard deviation; Wa = weighted average; Is. age = isochron age; Tot. age = total age; SH total age = step-heating integrated total age. The displayed errors do not include the uncertainty in FCTb standard age. The abbreviations in the stratigraphic age column are: MM = Middle Miocene; P = Pliocene; PP = Plio-Pleistocene. The last line of the table gives the average and standard deviation of the columns above.

size used. No temperature measuring devices are available on the system, so the temperatures at which these changes were observed are unknown. Step heating data, where available, are, therefore, used for integrated total ages only. A similar behavior, i.e., the formation of a sphere and a negligible release of gas until 1200°C, is also reported by Dalrymple et al. (1993) on dark brown to black impact glasses from the K/T boundary, Haiti, using a continuous Ar-ion laser as a heating device. Thus, this behavior seems to be characteristic of tektites and is not only due to the wavelength of the laser used to melt the sample.

The data were corrected for procedural blanks, mass discrimination, nuclear interferences, and $^{37}Ar$ and $^{39}Ar$ decay. The ages were calculated using the decay constants reported by Steiger and Jäger (1977): displayed errors are 1σ and are analytical errors unless otherwise stated. A conservative error of 0.5% was assigned to the irradiation factor J (Table 2).

Averages, weighted averages (all data points were inverse-variance weighted), and isochron calculations were performed on each sample individually (Table 1). In the isochron calculations, the low spread of data points resulting from the very high percentage of radiogenic $^{40}Ar$ was a limiting factor, leading to a considerable age spread and higher errors than occur with other methods of calculation. A different calculation approach was applied to the whole data set: each single chip analysis was considered to be an independent sample of a unique population, and the average, the weighted average, and the isochron were calculated. In this case, the errors associated with each single point also include the uncertainty in the irradiation factor J; the latter was propagated only after the internal routines of age calculations in individual samples, being a within-sample systematic error.

## DISCUSSION

Table 1 contains the results obtained with different types of calculation approaches, and Table 2 contains the $^{40}Ar/^{39}Ar$ analytical data. The apparent age variability within each sample is small, ranging between the 0.7% of Chlum, with its limited data set, and the 2.5% of Radomilice (the average for all the other samples is around 1–1.5%). Yields of radiogenic argon have a limited spread and are very high for all the samples; only Jankov#1 and Slavice display 1 point each with a higher atmospheric contamination and age values well within the interval of variation of the sample. The K/Ca ratios, which are calculated from the K-derived $^{39}Ar$ and the Ca-derived $^{37}Ar$, show values that, on average, are compatible with the chemical data for their respective strewn subfields and are not correlated with the age (Fig. 1). The lowest K/Ca ratio is from the K-poor Radomilice sample, while the highest is from the Ca-poor Slavice; the ratio of the latter is higher than the value obtained from average $K_2O$ and CaO contents

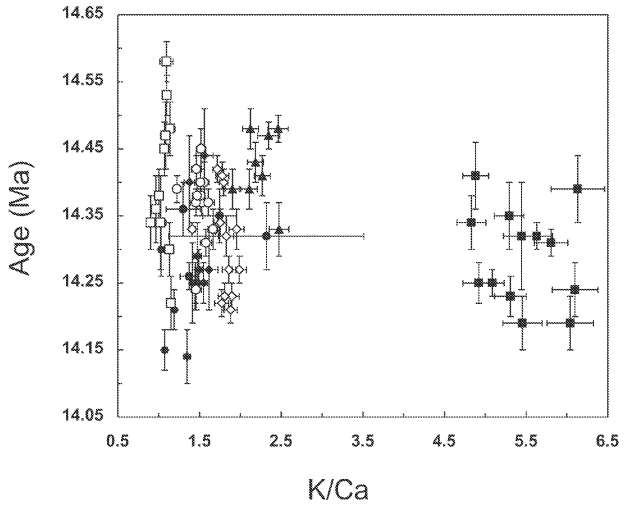


Fig. 1. Ages obtained from individual analyses are plotted versus the K/Ca ratio; displayed errors are ±1σ. Slavice: solid squares; Radomilice: empty squares; Chlum: solid circles; Vrábče: empty circles; Jankov#1: solid diamonds; Jankov#2: empty diamonds; Třebanice: solid triangles.

in the Moravian subfield (Bouška 1998) but is at the boundary of the interval of variation observed for these elements in the subfield (Koeberl 1986).

The averages vary between 14.27 and 14.42 Myr, which is a slightly smaller interval than was observed for the weighted averages (14.24–14.43 Myr) and total ages (that are the sum of all chips analyzed, 14.26–14.43 Myr). The average ages of samples from the second irradiation package (Jankov#2, Vrábče, Třebanice, and Radomilice) are slightly older than those of the first package. The age difference between the 2 samples from the Jankov deposit is, however, 40 ka, i.e., of the order of an average 2σ analytical error on a single measurement and, hence, is not significant. Isochron ages vary more, from 14.13 to 14.62 Myr, but this is also a consequence of the small spread of points. Age calculations using different approaches for each sample agree well, within error. None of the differences are related to sample provenances or stratigraphic ages. Calculations of the averages of individual sample averages, weighted averages, and total ages (last line in Table 1) give the same age (14.34 Myr) with different standard deviations. The last column of Table 1 gives, for comparison, the integrated total ages derived from step-heating measurements, where available. To account for any overestimation of applied errors mainly due to the uncertainty in vertical neutron flux variation, a weighted average calculation routine was run, assigning arbitrary and decreasing errors to the average ages of individual samples. Application of a 1σ error of 0.35% still gave a satisfactory MSWD (1.3), confirming that the analyzed samples belong to a unique population. The average of the samples average, 14.34 ± 0.06 Myr (standard deviation), gives a good estimate of the age of moldavites.

Table 2. $^{40}Ar/^{39}Ar$ laser total fusion analytical data.[a]

| ID #run | $^{36}Ar_{(a)}$ | $^{37}Ar_{(Ca)}$ | $^{38}Ar_{(Cl)}$ | $^{39}Ar_{(K)}$ | $^{40}Ar_{(r)}$ | Age (Myr) | ±1σ | $^{40}Ar_{(r)}$ (%) | K/Ca | ±1σ |
|---|---|---|---|---|---|---|---|---|---|---|
| Slavice | J = 0.000877 ± 0.0000044 | | | | | | | | | |
| PAV49–10#1 | 1.53E–14 | 6.86E–12 | b.d.l. | 6.25E–11 | 5.69E–10 | 14.34 | ± 0.04 | 99.1 | 4.83 | 0.18 |
| PAV49–10#2 | 1.69E–14 | 5.92E–12 | b.d.l. | 5.93E–11 | 5.35E–10 | 14.23 | ± 0.03 | 99.0 | 5.31 | 0.19 |
| PAV49–10#3 | 1.88E–14 | 3.73E–12 | b.d.l. | 4.32E–11 | 3.94E–10 | 14.39 | ± 0.05 | 98.5 | 6.13 | 0.33 |
| PAV49–10#4 | 2.95E–14 | 4.51E–12 | b.d.l. | 5.19E–11 | 4.69E–10 | 14.24 | ± 0.04 | 98.1 | 6.10 | 0.28 |
| PAV49–10#5 | 5.16E–15 | 1.95E–12 | b.d.l. | 2.22E–11 | 2.00E–10 | 14.19 | ± 0.04 | 99.1 | 6.04 | 0.29 |
| PAV49–10#6 | 2.72E–14 | 1.01E–11 | 9.03E–15 | 9.70E–11 | 8.77E–10 | 14.25 | ± 0.02 | 99.0 | 5.08 | 0.15 |
| PAV49–10#7 | 1.08E–14 | 4.55E–12 | b.d.l. | 4.22E–11 | 3.82E–10 | 14.25 | ± 0.03 | 99.0 | 4.92 | 0.19 |
| PAV49–10#8 | 3.10E–14 | 6.64E–12 | b.d.l. | 6.12E–11 | 5.59E–10 | 14.41 | ± 0.05 | 98.3 | 4.88 | 0.16 |
| PAV49–10#9 | 2.44E–13 | 6.71E–12 | b.d.l. | 6.70E–11 | 6.10E–10 | 14.35 | ± 0.05 | 89.3 | 5.29 | 0.18 |
| PAV49–10#10 | 1.31E–14 | 3.18E–12 | b.d.l. | 3.26E–11 | 2.96E–10 | 14.32 | ± 0.08 | 98.6 | 5.44 | 0.22 |
| PAV49–10#11 | 2.92E–14 | 4.73E–12 | b.d.l. | 5.02E–11 | 4.56E–10 | 14.32 | ± 0.02 | 98.0 | 5.63 | 0.19 |
| PAV49–10#12 | 1.84E–14 | 5.99E–12 | 1.07E–15 | 6.56E–11 | 5.96E–10 | 14.31 | ± 0.02 | 99.0 | 5.81 | 0.21 |
| PAV49–10#13 | 1.03E–14 | 3.86E–12 | 2.13E–15 | 3.98E–11 | 3.58E–10 | 14.19 | ± 0.04 | 99.0 | 5.46 | 0.24 |
| Jankov#1 | J = 0.000869 ± 0.0000043 | | | | | | | | | |
| PAV49–7#1 | 1.34E–14 | 1.50E–11 | b.d.l. | 3.81E–11 | 3.45E–10 | 14.14 | ± 0.04 | 98.7 | 1.35 | 0.04 |
| PAV49–7#2 | 4.32E–14 | 2.87E–11 | 4.28E–15 | 6.45E–11 | 5.87E–10 | 14.21 | ± 0.03 | 97.8 | 1.19 | 0.03 |
| PAV49–7#3 | 1.29E–14 | 1.75E–11 | b.d.l. | 4.93E–11 | 4.51E–10 | 14.27 | ± 0.03 | 99.0 | 1.49 | 0.04 |
| PAV49–7#4 | 3.53E–14 | 1.92E–11 | 3.37E–13 | 5.62E–11 | 5.12E–10 | 14.25 | ± 0.03 | 97.9 | 1.55 | 0.05 |
| PAV49–7#5 | 4.38E–14 | 2.58E–11 | b.d.l. | 7.05E–11 | 6.43E–10 | 14.24 | ± 0.03 | 97.9 | 1.44 | 0.04 |
| PAV49–7#6 | 1.33E–14 | 9.06E–12 | 9.43E–14 | 2.52E–11 | 2.31E–10 | 14.29 | ± 0.05 | 98.2 | 1.48 | 0.05 |
| PAV49–7#7 | 2.88E–14 | 3.81E–11 | b.d.l. | 1.04E–10 | 9.50E–10 | 14.25 | ± 0.03 | 99.0 | 1.45 | 0.04 |
| PAV49–7#8 | 2.65E–14 | 1.25E–11 | b.d.l. | 2.53E–11 | 2.29E–10 | 14.15 | ± 0.03 | 96.6 | 1.08 | 0.03 |
| PAV49–7#9 | 6.03E–14 | 6.23E–11 | 9.03E–14 | 1.21E–10 | 1.11E–09 | 14.30 | ± 0.04 | 98.3 | 1.03 | 0.03 |
| PAV49–7#10 | 2.71E–14 | 2.86E–11 | 3.13E–15 | 7.64E–11 | 6.97E–10 | 14.25 | ± 0.06 | 98.7 | 1.42 | 0.04 |
| PAV49–7#11 | 4.43E–14 | 5.72E–12 | b.d.l. | 1.75E–11 | 1.60E–10 | 14.27 | ± 0.06 | 92.3 | 1.62 | 0.11 |
| PAV49–7#12 | 2.03E–14 | 5.81E–12 | 3.90E–15 | 1.71E–11 | 1.58E–10 | 14.44 | ± 0.07 | 96.2 | 1.56 | 0.10 |
| PAV49–7#13 | 3.93E–14 | 1.26E–11 | b.d.l. | 3.29E–11 | 3.03E–10 | 14.40 | ±0.07 | 96.2 | 1.38 | 0.06 |
| Chlum | J = 0.000882 ± 0.0000044 | | | | | | | | | |
| PAV49–12#1 | 1.34E–14 | 1.55E–11 | b.d.l. | 5.11E–11 | 4.62E–10 | 14.35 | ± 0.04 | 99.0 | 1.75 | 0.21 |
| PAV49–12#2 | 4.08E–15 | 9.88E–12 | 3.86E–15 | 2.43E–11 | 2.20E–10 | 14.36 | ± 0.04 | 99.3 | 1.30 | 0.21 |
| PAV49–12#3 | 2.77E–15 | 2.71E–12 | b.d.l. | 1.18E–11 | 1.07E–10 | 14.32 | ± 0.05 | 99.1 | 2.32 | 1.20 |
| PAV49–12#4 | 1.42E–14 | 3.66E–11 | b.d.l. | 9.50E–11 | 8.55E–10 | 14.26 | ± 0.02 | 99.4 | 1.37 | 0.11 |
| Jankov#2 | J = 0.000592 ± 0.000003 | | | | | | | | | |
| PAV51–28#1 | b.d.l. | 1.24E–11 | b.d.l. | 4.01E–11 | 5.43E–10 | 14.42 | ± 0.02 | 99.9 | 1.72 | 0.06 |
| PAV51–28#2 | 1.14E–14 | 6.45E–11 | 6.20E–14 | 1.71E–10 | 2.31E–09 | 14.33 | ± 0.01 | 99.8 | 1.41 | 0.04 |
| PAV51–28#3 | 1.67E–14 | 4.95E–11 | 4.79E–15 | 1.68E–10 | 2.27E–09 | 14.40 | ± 0.02 | 99.7 | 1.80 | 0.05 |
| PAV51–28#4 | 1.12E–14 | 3.35E–11 | 7.33E–14 | 1.07E–10 | 1.44E–09 | 14.33 | ± 0.01 | 99.7 | 1.70 | 0.05 |
| PAV51–28#5 | 3.73E–15 | 1.56E–11 | b.d.l. | 5.48E–11 | 7.36E–10 | 14.27 | ± 0.02 | 99.8 | 1.86 | 0.08 |
| PAV51–28#6 | 9.60E–15 | 1.73E–11 | 2.00E–14 | 5.73E–11 | 7.72E–10 | 14.34 | ± 0.02 | 99.6 | 1.75 | 0.08 |
| PAV51–28#7 | 5.61E–15 | 1.68E–11 | 3.26E–14 | 5.65E–11 | 7.65E–10 | 14.41 | ± 0.02 | 99.7 | 1.78 | 0.08 |
| PAV51–28#8 | 9.06E–15 | 9.48E–12 | 1.15E–14 | 3.27E–11 | 4.40E–10 | 14.32 | ± 0.03 | 99.3 | 1.83 | 0.09 |
| PAV51–28#9 | 1.07E–14 | 1.50E–11 | 2.69E–15 | 5.36E–11 | 7.17E–10 | 14.23 | ± 0.02 | 99.5 | 1.90 | 0.09 |
| PAV51–28#10 | 1.03E–14 | 1.36E–11 | 2.87E–14 | 4.64E–11 | 6.21E–10 | 14.23 | ± 0.02 | 99.4 | 1.81 | 0.08 |
| PAV51–28#11 | 1.60E–14 | 2.42E–11 | 1.77E–14 | 8.60E–11 | 1.15E–09 | 14.21 | ± 0.02 | 99.5 | 1.88 | 0.08 |
| PAV51–28#12 | 6.53E–15 | 1.01E–11 | b.d.l. | 3.74E–11 | 5.04E–10 | 14.33 | ± 0.03 | 99.5 | 1.96 | 0.09 |
| PAV51–28#13 | 8.99E–15 | 1.22E–11 | 7.88E–15 | 4.06E–11 | 5.43E–10 | 14.22 | ± 0.02 | 99.4 | 1.77 | 0.09 |
| PAV51–28#14 | 1.37E–14 | 1.66E–11 | 7.32E–15 | 6.23E–11 | 8.36E–10 | 14.27 | ± 0.02 | 99.4 | 1.99 | 0.09 |
| Radomilice | J = 0.000581 ± 0.0000029 | | | | | | | | | |
| PAV51–32#1 | 5.28E–15 | 1.25E–11 | b.d.l. | 2.28E–11 | 3.14E–10 | 14.36 | ± 0.05 | 99.4 | 0.97 | 0.05 |
| PAV51–32#2 | 7.91E–15 | 1.24E–11 | 2.64E–14 | 2.51E–11 | 3.48E–10 | 14.45 | ± 0.04 | 99.3 | 1.07 | 0.05 |
| PAV51–32#3 | 8.74E–15 | 9.36E–12 | 2.24E–15 | 2.03E–11 | 2.76E–10 | 14.22 | ± 0.04 | 99.0 | 1.15 | 0.05 |
| PAV51–32#4 | 6.41E–14 | 1.77E–11 | b.d.l. | 3.36E–11 | 4.63E–10 | 14.38 | ± 0.04 | 96.0 | 1.01 | 0.04 |
| PAV51–32#5 | 5.49E–15 | 1.62E–11 | 1.34E–14 | 3.36E–11 | 4.68E–10 | 14.53 | ± 0.03 | 99.6 | 1.10 | 0.05 |
| PAV51–32#6 | 1.80E–14 | 1.71E–11 | 1.50E–14 | 3.66E–11 | 5.01E–10 | 14.30 | ± 0.04 | 98.9 | 1.13 | 0.05 |
| PAV51–32#7 | 5.52E–15 | 7.42E–12 | 5.97E–15 | 1.43E–11 | 1.96E–10 | 14.34 | ± 0.07 | 99.1 | 1.02 | 0.07 |
| PAV51–32#8 | 2.84E–14 | 1.80E–11 | b.d.l. | 3.07E–11 | 4.21E–10 | 14.34 | ± 0.04 | 98.0 | 0.90 | 0.04 |
| PAV51–32#9 | 1.25E–15 | 1.18E–11 | 2.15E–14 | 2.54E–11 | 3.53E–10 | 14.48 | ± 0.04 | 99.8 | 1.14 | 0.06 |
| PAV51–32#10 | 6.42E–15 | 1.01E–11 | b.d.l. | 2.07E–11 | 2.87E–10 | 14.47 | ± 0.05 | 99.3 | 1.08 | 0.06 |

Table 2. $^{40}Ar/^{39}Ar$ laser total fusion analytical data.[a] *Continued.*

| ID #run | $^{36}Ar_{(a)}$ | $^{37}Ar_{(Ca)}$ | $^{38}Ar_{(Cl)}$ | $^{39}Ar_{(K)}$ | $^{40}Ar_{(r)}$ | Age (Myr) | ±1σ | $^{40}Ar_{(r)}$ (%) | K/Ca | ±1σ |
|---|---|---|---|---|---|---|---|---|---|---|
| PAV51–32#11 | b.d.l. | 6.41E–12 | 1.54E–14 | 1.32E–11 | 1.85E–10 | 14.58 | ± 0.03 | 99.9 | 1.09 | 0.08 |
| Třebanice | J = 0.000575 ± 0.0000029 | | | | | | | | | |
| PAV51–34#1 | 5.98E–15 | 6.71E–12 | 1.48E–14 | 2.41E–11 | 3.35E–10 | 14.39 | ± 0.03 | 99.4 | 1.90 | 0.09 |
| PAV51–34#2 | 1.05E–14 | 1.06E–11 | b.d.l. | 4.94E–11 | 6.92E–10 | 14.48 | ± 0.02 | 99.5 | 2.46 | 0.12 |
| PAV51–34#3 | 1.15E–14 | 9.54E–12 | 1.26E–14 | 4.22E–11 | 5.92E–10 | 14.47 | ± 0.02 | 99.4 | 2.35 | 0.14 |
| PAV51–34#4 | 5.87E–15 | 7.64E–12 | 1.41E–15 | 3.07E–11 | 4.29E–10 | 14.48 | ± 0.03 | 99.5 | 2.13 | 0.10 |
| PAV51–34#5 | 6.50E–15 | 6.82E–12 | 5.17E–15 | 3.18E–11 | 4.42E–10 | 14.33 | ± 0.04 | 99.5 | 2.47 | 0.12 |
| PAV51–34#6 | 2.16E–15 | 8.32E–12 | 7.89E–15 | 3.31E–11 | 4.61E–10 | 14.39 | ± 0.03 | 99.8 | 2.11 | 0.10 |
| PAV51–34#7 | 4.23E–15 | 9.37E–12 | 1.41E–14 | 3.86E–11 | 5.40E–10 | 14.43 | ± 0.03 | 99.7 | 2.18 | 0.10 |
| PAV51–34#8 | 8.10E–15 | 1.12E–11 | 1.91E–14 | 4.79E–11 | 6.68E–10 | 14.41 | ± 0.03 | 99.6 | 2.27 | 0.10 |
| Vrábče | J = 0.000583 ± 0.0000029 | | | | | | | | | |
| PAV51–31#1 | 7.06E–15 | 1.27E–11 | 1.52E–14 | 3.49E–11 | 4.75E–10 | 14.24 | ± 0.03 | 99.5 | 1.46 | 0.06 |
| PAV51–31#2 | 1.34E–14 | 1.63E–11 | b.d.l. | 4.71E–11 | 6.47E–10 | 14.37 | ± 0.02 | 99.3 | 1.53 | 0.07 |
| PAV51–31#3 | 1.71E–14 | 2.65E–11 | 3.37E–15 | 7.30E–11 | 1.01E–09 | 14.42 | ± 0.02 | 99.4 | 1.46 | 0.06 |
| PAV51–31#4 | 1.13E–14 | 2.16E–11 | 1.82E–14 | 6.55E–11 | 8.99E–10 | 14.37 | ± 0.02 | 99.6 | 1.61 | 0.07 |
| PAV51–31#5 | 1.70E–14 | 3.63E–11 | 2.42E–14 | 1.08E–10 | 1.48E–09 | 14.31 | ± 0.02 | 99.6 | 1.58 | 0.07 |
| PAV51–31#6 | 1.03E–14 | 1.49E–11 | b.d.l. | 4.10E–11 | 5.62E–10 | 14.37 | ± 0.02 | 99.4 | 1.46 | 0.07 |
| PAV51–31#7 | 8.66E–15 | 2.59E–11 | 1.97E–14 | 5.99E–11 | 8.23E–10 | 14.39 | ± 0.02 | 99.6 | 1.22 | 0.05 |
| PAV51–31#8 | 2.86E–14 | 3.44E–11 | 5.99E–15 | 1.01E–10 | 1.39E–09 | 14.40 | ± 0.03 | 99.3 | 1.56 | 0.06 |
| PAV51–31#9 | 1.66E–14 | 1.61E–11 | 5.29E–14 | 4.60E–11 | 6.35E–10 | 14.45 | ± 0.03 | 99.2 | 1.52 | 0.06 |
| PAV51–31#10 | 2.14E–14 | 2.25E–11 | 1.05E–14 | 6.47E–11 | 8.92E–10 | 14.45 | ± 0.03 | 99.2 | 1.52 | 0.05 |
| PAV51–31#11 | 5.62E–14 | 1.49E–11 | 2.82E–14 | 4.68E–11 | 6.41E–10 | 14.33 | ± 0.03 | 97.4 | 1.66 | 0.06 |
| PAV51–31#12 | 3.53E–14 | 6.20E–11 | 2.03E–15 | 1.77E–10 | 2.43E–09 | 14.38 | ± 0.01 | 99.5 | 1.52 | 0.05 |
| PAV51–31#13 | 4.25E–14 | 2.29E–11 | 3.08E–14 | 6.35E–11 | 8.71E–10 | 14.38 | ± 0.02 | 98.5 | 1.47 | 0.06 |
| PAV51–31#14 | 2.52E–14 | 4.20E–11 | 1.85E–14 | 1.20E–10 | 1.64E–09 | 14.40 | ± 0.02 | 99.5 | 1.51 | 0.05 |

[a] Amounts of all isotopes are expressed as ccSTP. The errors in ages are analytical and do not include the uncertainty in the factor J. $^{36}Ar_{(a)}$ = atmospheric $^{36}Ar$; $^{37}Ar_{(Ca)}$ = Ca-derived $^{37}Ar$; $^{38}Ar_{(Cl)}$ = Cl-derived $^{38}Ar$; $^{39}Ar_{(K)}$ = K-derived $^{39}Ar$; $^{40}Ar_{(r)}$ = radiogenic $^{40}Ar$; $^{40}Ar_{(r)}$(%) = percentage of radiogenic $^{40}Ar$; b.d.l. = below detection limit. Ar isotope corrections for interfering neutron reactions are: $^{40}Ar_K/^{39}Ar_K = 0.0112 \pm 0.0022$ (PAV49) and $0.0096 \pm 0.0019$ (PAV51); $^{39}Ar_{Ca}/^{37}Ar_{Ca} = 0.00075 \pm 0.00006$ (PAV49) and $0.00075 \pm 0.00008$ (PAV51); $^{36}Ar_{Ca}/^{37}Ar_{Ca} = 0.00024 \pm 0.000024$.

All $^{40}Ar/^{39}Ar$ ages are relative to an age standard, and values from 27.42 to 28.03 Myr have been quoted for the FCT biotite and sanidine standards using different calibration approaches (see Villeneuve et al. [2000] for a thorough review). FCTb (split 3) has been used here, with an age of 27.95 ± 0.09 Myr (1σ) (Baksi et al. 1996) that was derived from an $^{40}Ar/^{39}Ar$ intercalibration with some widespread standards. The age of the moldavites would decrease and increase by 0.27 and 0.04 Myr, respectively, considering the above interval of variation on the age of the standard. The uncertainty in the standard deviation of the average is ±0.08 Myr considering a 1σ error in the age of FCTb.

In a completely different approach, all the analyzed chips were considered as independent samples, and the above calculations were applied to the 77 data points. The data were plotted as a cumulative probability distribution diagram coupled with a histogram the bin width of which is equal to the average error of individual points (Fig. 2). The overall result does not change: the average and its standard deviation is 14.37 ± 0.09 Myr and the weighted average is 14.34 ± 0.02 Myr (2σ) with a MSWD = 0.72. The isochron age is 14.32 ± 0.03 Myr (2σ, MSWD = 0.56) with a $^{40}Ar/^{36}Ar$ intercept of 291 ± 31. The atmospheric value is within error (Fig. 3). The uncertainty in sample ages derived from the uncertainty in the age of the standard and from the analytical error is ±0.09 and ±0.10 Myr (2σ) on the weighted average and isochron ages, respectively. The uncertainty in the standard deviation of the average is ±0.10 Myr, considering a 1σ error in the age of FCTb.

Comparisons of published $^{40}Ar/^{39}Ar$ data should take into account both the age used for the standard and any cross-calibrations available for the different standards. The ages obtained in this paper using different calculation approaches are all younger than the 15.21 ± 0.15 Myr of Staudacher et al. (1982: age monitor B4M, 18.5 ± 0.2 Myr) and are much more precise than the 15.1 ± 2.1 (1σ) and 14.2 ± 2.1 (1σ) Myr of Mader et al. (2001: age monitor B4M, 18.6 ± 0.4 Myr). Baksi et al. (1996) recommend a value of 18.51 Myr for B4M, and they obtained an age of 18.54 ± 0.05 Myr (1σ) versus 27.95 Myr for FCTb. The ages displayed here are equal within error to the 14.4 ± 0.25 Myr (Lange et al. 1995; recalculated at 14.52 ± 0.40 Myr in Schwarz and Lippolt [2002]) of a moldavite from Lusatia and to recent ages on Lusatian and Bohemian samples (14.38 ± 0.44 Myr and 14.50 ± 0.42 Myr, respectively, 2σ error; Schwarz and Lippolt 2002). These data were obtained using the age monitor HD-B1 bt, with an assigned age of 24.21 ± 0.32 Myr (1σ) (Hess and Lippolt 1994), and no cross-calibration of HD-B1 bt relative to FCTb exists.

## CONCLUSIONS

An age of 14.34 ± 0.08 Myr, which represents the average of individual sample averages and total ages and is

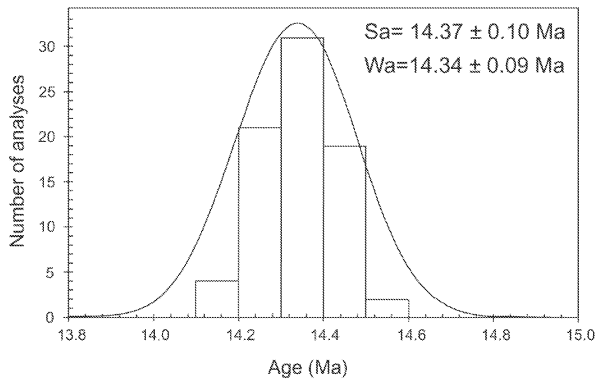


Fig. 2. Cumulative probability distribution diagram. All individual $^{40}Ar/^{39}Ar$ laser fusion data points were used in this diagram. The cumulative probability distribution is plotted with a histogram of the data included in the plot. The bin width is equal to the average error of data points, 0.1 Myr. Sa = average ± standard deviation. Wa = weighted average ±2σ. The errors in the average and weighted average comprise the uncertainty in the age of the standard.

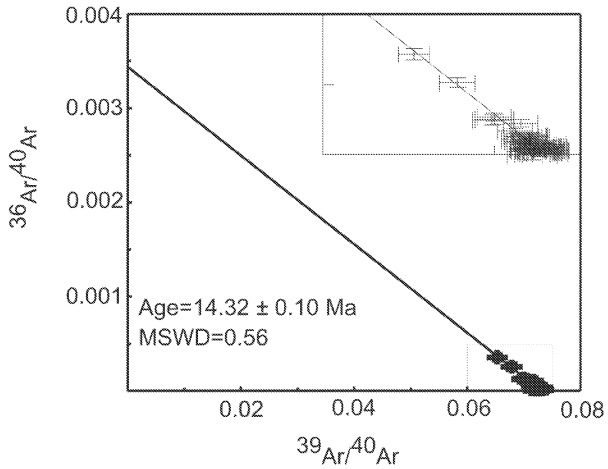


Fig. 3. Isochron diagram of individual $^{40}Ar/^{39}Ar$ laser total fusion analyses of moldavite chips. The data point error symbol is ±1σ. The error in the age and the intercept value is at the ±2σ level; the former comprises the uncertainty in the age of the standard. The y-axis intercept (0.003436 ± 0.000336) will translate to an initial $^{40}Ar/^{36}Ar$ ratio of 291 ± 31. The insert at the top represents a magnified version of the area in the main field of the diagram.

equivalent to all ages obtained with the "one fusion, one sample" approach, may be considered the best estimate of the age of the Central European tektite strewn field. This value is related to the age of the monitor FCTb, 27.95 ± 0.09 Myr (1σ); the displayed error on the moldavite age represents the standard deviation of the average plus the 1σ error in monitor calibration. No age differences were observed in samples from distinct subfields or different stratigraphic ages. A good calibration has thus been achieved for this FT reference glass.

This new datum constrains the age of a tektite field devoid of stratigraphic control and allows us to search for signs of its impact-forming event, such as glass spherules or shocked minerals, in marine sedimentary series far from the outcrop area (Mader et al. 2001). The 2 more detailed and recent time scales of the Miocene (Berggren et al. 1995; Odin et al. 1997) were obtained using different age standards from the one used here: FCT sanidine and HD-B1 biotite. Assuming that sanidine and biotite of the same unit, Fish Canyon Tuff ignimbrite, are coeval, which is a reasonable assumption for a volcanic rock, and applying a correction for the different calibration of age standards, we can recalculate the moldavite age relative to FCT sanidine at 27.84 Myr, which is used in the Berggren et al. (1995) time scale. The value obtained, 14.28 Myr, places moldavite formation in the Lower Serravallian.

The Central Europe strewn field has been associated, on the basis of its geographic position and chronological data, with the nearby Nördlinger Ries impact crater. The revised age for the strewn field presented here is younger than the most commonly accepted age for the crater: the $^{40}Ar/^{39}Ar$ plateau age of 15.0 ± 0.5 Myr (Staudacher et al. 1982). All literature data on suevitic glasses from the Ries are around 15 Myr, similar to the moldavites (Gentner et al. 1967; Bogard et al. 1988; Mader et al. 2001), but they have high errors and are much more scattered. This observation is consistent with the fact that the dating of impact melt layers is more problematic because of the frequent partial resetting of the system during the forming event and/or because of secondary alteration processes (Deutsch and Schärer 1994). Tektites, on the other hand, are considered almost ideal samples and, when unaltered, give very precise ages (Deutsch and Schärer 1994). A recently published paper reports ages that are younger than previous data for Ries glasses, giving a mean apparent age for glass particles of 14.3 ± 0.1 Myr (2σ), relative to an age of the standard Taylor Creek Rhyolite sanidine (TCRs) of 27.92 Myr (Buchner et al. 2003). An age difference of 0.1 Myr between TCRs and FCTb has been reported, with TCRs being the older of the two (van den Bogaard 1995). Taking into account this cross-calibration, the glass particles' age will increase by about 0.07 Myr relative to FCTb. In another calibration, TCRs is 0.3 Myr older than FCTb (Renne et al. 1998), further increasing the age of the Ries glass particles. However, their age remains equal to, within the 2σ error, the moldavite age obtained in this paper. If the genetic link between the moldavites and Ries crater is accepted, then the age obtained for the Central European tektite strewn field gives a better estimate of the crater age.

*Acknowledgments*–This paper is dedicated to the memory of Vladimir Bouška, who died during work on this study. We would like to thank J. Gilmour for his helpful comments on an earlier version of the manuscript, as well as W. Schwarz, D. Mader, and C. Koeberl for their careful reviews of the manuscript. We are also grateful to the Associate Editor R. Wieler for his advice. The Italian National Antarctic Research Program funded the $^{40}Ar/^{39}Ar$ laser probe facility at the IGG-CNR in Pisa.

*Editorial Handling*—Dr. Rainer Wieler

## REFERENCES


Baksi A. K., Archibald D. A., and Farrar E. 1996. Intercalibration of $^{40}Ar/^{39}Ar$ dating standards. *Chemical Geology* 129:307–324.

Balestrieri M. L., Bigazzi G., and Bouška V. 1997. Jankov moldavite: A potential glass standard for fission-track dating. *On Track* 7: 13–16.

Balestrieri M. L., Bigazzi G., Bouška V., Labrin E., Hadler J. C., Kitada N., Osorio A. M., Poupeau G., Wadatsumi K., and Zuñiga A. G. 1998. Potential glass age standards for fission-track dating: An overview. In *Advances in fission-track geochronology,* edited by Van den haute P. and De Corte F. Dordrecht: Kluwer Academic Publishers. pp. 287–304.

Berggren W. A., Kent D. V., Swisher C. C., III, and Aubry M. P. 1995. A revised Cenozoic geochronology and chronostratigraphy. *Geochronology time scales and global stratigraphic correlation.* SEPM Special Publication No. 54. pp. 129–212.

Bigazzi G. and De Michele V. 1996. New fission-track age determinations on impact glasses. *Meteoritics & Planetary Science* 31:234–236.

Bogard D., Hörz F., and Stöffler D. 1988. Loss of radiogenic argon from shocked granitic clasts in suevite deposits from the Ries crater. *Geochimica and Cosmochimica Acta* 52:2639–2649.

Bouška V. 1998. The Moldavite strewn field. *Chemie der Erde* 58: 321–343.

Bouška V., Balestrieri M. L., Bigazzi G., and Laurenzi M. A. 2000. Moldavite: An age standard for fission-track dating. *Bulletin of the Czech Geological Survey* 75:105–114.

Buchner E., Seyfried H., and van den Bogaard P. 2003. $^{40}Ar/^{39}Ar$ laser probe age determination confirms the Ries impact crater as the source of glass particles in Graupensand sediments (Grimmelfingen Formation, North Alpine Foreland Basin). *International Journal of Earth Sciences* 92:1–6.

Dalrymple G. B., Izett G. A., Snee L. W., and Obradovick J. D. 1993. $^{40}Ar/^{39}Ar$ age spectra and total-fusion ages of tektites from Cretaceous-Tertiary boundary sedimentary rocks in the Beloc Formation, Haiti. *United States Geological Survey Bulletin* 2065: 1–20.

Deutsch A. and Schärer U. 1994. Dating terrestrial impact events. *Meteoritics* 29:301–322.

Dressler B. O. and Reimold W. U. 2001. Terrestrial impact melt rocks and glasses. *Earth Science Reviews* 56:205–284.

Gentner W., Lippolt H. J., and Schaeffer O. A. 1963. Argonbestimmungen an Kaliummineralien—XI: Die kalium-argon-alter der Gläser des Nördlingen Rieses und der böhmisch-mährischen tektite. *Geochimica and Cosmochimica Acta* 27: 191–200.

Gentner W., Kleinman B., and Wagner G. A. 1967. New K/Ar and fission track ages of impact glasses and tektites. *Earth and Planetary Science Letters* 2:83–86.

Grieve R. A. F. 1997. Extraterrestrial impact events: The record in the rocks and the stratigraphic column. *Paleogeography, Paleoclimatology, Paleoecology* 132:5–23.

Hess J. C. and Lippolt H. J. 1994. Compilation of K-Ar measurements on HD-B1 standard Biotite—1994 status report. *Bulletin of Liaison and Informations* 12:19–23.

Hurford A. J. 1990. International Union of Geological Sciences. Subcommission on Geochronology. Recommendation for the standardization of fission track dating calibration and data reporting. *Nuclear Tracks and Radiation Measurements* 17:233–236.

Koeberl C. 1986. Geochemistry of tektites and impact glasses. *Annual Review of Earth and Planetary Sciences* 14:323–350.

Koeberl C. 1994. Tektite origin by hypervelocity asteroidal or cometary impact: Target rocks, source craters, and mechanism. In *Large meteorite impacts and planetary evolution,* edited by Dressler B. O., Grieve R. A. F., and Sharpton V. L. Boulder: Geological Society of America Special Paper 293. pp. 133–151.

Lange J. M., Bollinger K., Horn P., Jessberger E. K., Schaaf P., Storzer D. 1995. Moldavites from Lusatia (Germany) III: Sr-isotope, $^{40}Ar/^{39}Ar$, and fission track studies. 26th Lunar and Planetary Science Conference. pp. 823–824.

Mader D., Montanari A., Gattacceca J., Koeberl C., Handler R., and Coccioni R. 2001. $^{40}Ar/^{39}Ar$ dating of Langhian biotite-rich clay layer in the pelagic sequence of the Cònero Riviera, Ancona, Italy. *Earth and Planetary Science Letters* 194:111–126.

McDougall I. and Lovering J. F. 1969. Apparent K-Ar dates on cores and excess Ar in flanges of australites. *Geochimica and Cosmochimica Acta* 33:1057–1070.

Odin G. S., Montanari A., and Coccioni R. 1997. Chronostratigraphy of Miocene stages: A proposal for the definition of precise boundaries. In *Miocene stratigraphy: An integrated approach,* edited by Montanari A., Odin G. S., and Coccioni R. Amsterdam: Elsevier. pp. 597–629.

Renne P. R., Swisher C. C., Deino A. L., Owens T. L., DePaolo D. J., and Karner D. B. 1998. Intercalibration of standards, absolute ages, and uncertainties in $^{40}Ar/^{39}Ar$ dating. *Chemical Geology* 145:117–152.

Schwarz W. H. and Lippolt H. J. 2002. Coeval $^{40}Ar/^{39}Ar$ ages of moldavites from the Bohemian and Lusatian strewn fields. *Meteoritics & Planetary Science* 37:1757–1763.

Staudacher T., Jessberger E. K., Dominik B., Kirsten T., Schaeffer O. A. 1982. $^{40}Ar/^{39}Ar$ ages of rocks and glasses from the Nördlinger Ries crater and the temperature history of impact breccias. *Journal of Geophysics* 51:1–11.

Steiger R. H. and Jäger E. 1977. Subcommission on Geochronology: Convention on the use of decay constants in geo- and cosmochronology. *Earth and Planetary Science Letters* 36:359–362.

Storzer D., Jessberger E. K., Kunz J., and Lange J. M. 1995. Synopsis von spaltspuren- und kalium-argon-datierungen an Ries-Impactglasern und Moldaviten. Exkursf. u. Veröfftl. *Gesellschaft für Geowissenschaften* 195:79–80.

Suess H. E., Hayden R. L., and Inghram M. G. 1951. Ages of tektites. *Nature* 168:432.

van den Bogaard P. 1995. $^{40}Ar/^{39}Ar$ ages of sanidine phenocrysts from Laacher See Tephra (12,900 yr BP): Chronostratigraphic and petrological significance. *Earth and Planetary Science Letters* 133:163–174.

Villeneuve M., Sandeman H. A., and Davis W. J. 2000. A method for intercalibration of U-Th-Pb and $^{40}Ar/^{39}Ar$ ages in the Phanerozoic. *Geochimica and Cosmochimica Acta* 64:4017–4030.

Zähringer J. 1963. K-Ar measurements of tektites. In *Radioactive dating. Proceedings NEA Symposium Athens, November 19–23.* Vienna: International Atomic Agency. pp. 289–305.